

Universal non-analytic behavior of the non-equilibrium Hall conductance in Floquet topological insulators

Markus Schmitt^{1,*} and Pei Wang²

¹*Institute for Theoretical Physics, Georg-August-Universität Göttingen - Friedrich-Hund-Platz 1, Göttingen 37077, Germany*

²*Department of Physics, Zhejiang Normal University - Jinhua 321004, China*

(Dated: April 9, 2021)

We study the Hall conductance in a Floquet topological insulator in the long time limit after sudden switches of the driving amplitude. Based on a high frequency expansion of the effective Hamiltonian and the micromotion operator we demonstrate that the Hall conductance as function of the driving amplitude follows universal non-analytic laws close to phase transitions that are related to conic gap closing points, namely a logarithmic divergence for gapped initial states and jumps of a definite height for gapless initial states. This constitutes a generalization of the results known for the static systems to the driven case.

I. INTRODUCTION

Since the experimental discovery and theoretical explanation of the quantum Hall effect [1, 2] the concept of topological order has gained great importance in condensed matter physics for the understanding of phase transitions that cannot be associated with symmetry breaking. The astonishingly robust integer quantization of the Hall conductance in units of the conductance quantum, $\sigma_{xy} = C e^2/h$, is due to the fact that $C \in \mathbb{Z}$ can be identified as a topological invariant of the underlying band structure, namely the Chern number. After Haldane's seminal proposal of a model system featuring a quantized Hall conductance in the absence of an external magnetic field [3] enormous experimental and theoretical efforts led to the discovery of a large variety of systems with similar topologically protected transport properties, which are today referred to as topological insulators (TIs) [4].

Following theoretical proposals [5, 6] a topological insulator was recently realized experimentally with ultracold fermions in a periodically shaken optical lattice [7]. Despite the absence of energy conservation such *Floquet* topological insulators (FTIs) can be characterized by the Chern number of an effective Hamiltonian and support edge modes [8]. This allows to tune the topological properties of the system by adjusting the external driving force and opens possibilities to investigate non-equilibrium signatures of topological insulators, which gained increasing theoretical attention lately [9–13]. Note, however, that in some aspects the behavior of FTIs can significantly differ from the known behavior of TIs, e.g., when considering the bulk-edge correspondence [14].

A situation that was studied recently by Dehghani et al. [10] is the measurement of the Hall conductance a long time after suddenly switching on the external driving force. The system is initially prepared in the ground

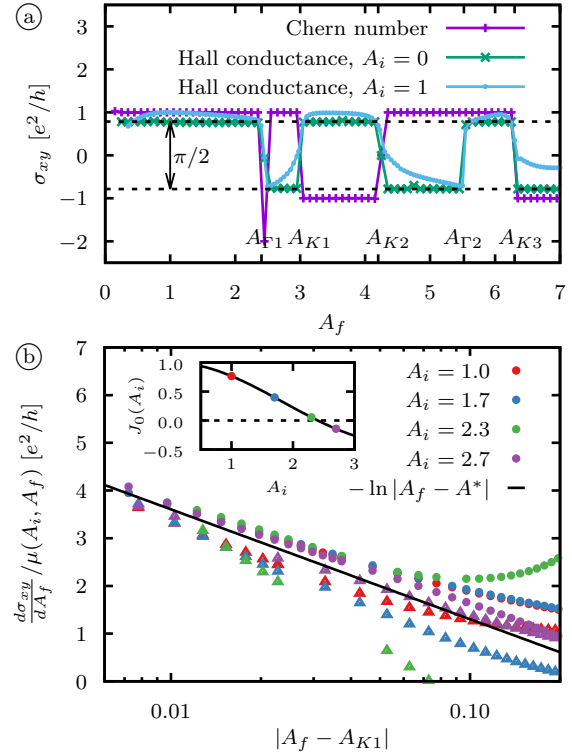


FIG. 1. a – Floquet Chern number C and non-equilibrium Hall conductance σ_{xy} for quenches with $A_i = 0$ and $A_i = 1$ as function of A_f for driving frequency $\omega = 10$. b – Derivative of the non-equilibrium Hall conductance rescaled by the prefactor $\mu(A_i, A_f) = J_0(A_f)|m_i|/J_0(A_i)m'_f$ determined in eq. (77) close to the transition at A_{K1} . As A_f approaches A_{K1} the slopes agree increasingly well with the predicted $\ln |A_f - A^*|$ (black line) in all cases even if the value $J_0(A_i)$ shown in the inset is small. Circles/triangles denote points to the left/right of K_1 .

state of the undriven Hamiltonian H_0 . Then the driving is suddenly switched on at time $t = 0$ and for $t > 0$ the system evolves under a time-periodic Hamiltonian $H_A(t)$, where A is the driving amplitude. The Hall conductance in the limit $t \rightarrow \infty$ is finally obtained using linear re-

* markus.schmitt@theorie.physik.uni-goettingen.de

sponse theory and a dephasing argument. As a result they numerically find for an electronic system that the post-quench Hall conductance, which is not any more an integer multiple of the conductance quantum, exhibits sudden changes whenever the post-quench Hamiltonian $H_A(t)$ crosses a topological phase boundary as function of the driving amplitude A . This behavior is very similar to the behavior of closed TIs after a quench, which exhibit a universal non-analytic behavior at the ground state transition of the final Hamiltonian as shown in Refs. [15, 16].

In this work we extend the analysis of closed TIs given in Refs. [15, 16] to FTIs. We analytically investigate the behavior of the Hall conductance after sudden switches of the driving amplitude for a tight binding Hamiltonian with a time periodic external potential. The analysis is based on high frequency expansions of the effective Hamiltonian and the micromotion operator. We focus on phase transitions that are associated with a closing of the quasi-energy gap at the K -points in the Brillouin zone. These already appear when only the first order contribution in the high frequency expansion of the effective Hamiltonian is considered. We find that suddenly switching on the driving amplitude from $A_i = 0$ to $A_f \neq 0$ with a gapless initial Hamiltonian leads to jumps of the Hall conductance by multiples of $\frac{\pi e^2}{2h}$ whenever A_f crosses a phase boundary, which agrees with the numerical results of Ref. [10] reproduced in Fig. 1a. If, instead, the system is initially prepared in a quasi-stationary Floquet mode of the initial Hamiltonian $H_{A_i}(t)$ before suddenly switching the driving amplitude to A_f the Hall conductance is continuous at critical values of A . Nevertheless, it is non-analytic with a logarithmically diverging derivative as a function of the driving amplitude A_f as shown in Fig. 1b.

A distinct feature of FTIs is the possible presence of so-called π -edge modes [17–20]. Note that our results do not apply to gap closings that affect these edge modes as discussed in section IV A.

The rest of the paper is divided into two parts. In section II we introduce the model system under consideration and briefly summarize the methods used and previous results, which are relevant for the further analysis. In section III we present our analysis resulting in the identification of the abovementioned non-analytic behavior of the Hall conductance, which is universal for conic gap-closing points in two-band FTIs.

II. BACKGROUND

In this section we introduce the model Hamiltonian under consideration and briefly review the Floquet formalism and the high frequency expansion used for our analysis. Moreover, we give a short summary of previous results on the non-equilibrium Hall conductance relevant for this work.

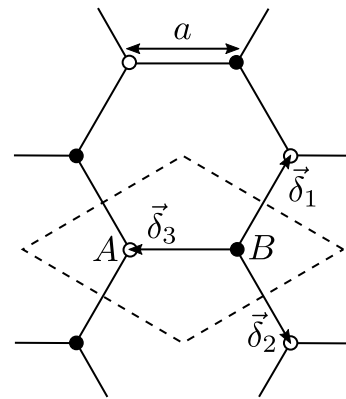


FIG. 2. We consider a hexagonal lattice structure. The dashed line marks a possible choice of the unit cell with two basis sites A and B . Depicted is moreover the unit of distance, a , and the nearest-neighbor vectors $\vec{\delta}_i$.

A. Model Hamiltonian

We consider a simple model Hamiltonian, namely a tight binding model on a hexagonal lattice subject to a time-periodic external potential,

$$\tilde{H}(t) = -t_h \sum_{\langle i,j \rangle} (c_i^\dagger c_j + h.c.) + \sum_i V(\vec{r}_i, t) c_i^\dagger c_i, \quad (1)$$

where $V(\vec{r}, t) = V_0 \vec{r} \cdot [-\cos(\omega t) \hat{e}_x + \sin(\omega t) \hat{e}_y]$ and $\langle i, j \rangle$ denotes the set of pairs of neighboring lattice sites. This Hamiltonian constitutes a simple description of graphene illuminated by a circularly polarized laser [21] or ultra-cold atoms in a circularly shaken optical lattice [7].

A time-dependent gauge transformation restores translational invariance and allows to write the Hamiltonian in momentum space as

$$H(t) = \sum_{\vec{k}} \vec{c}_{\vec{k}}^\dagger \left[\vec{d}_{\vec{k}}(t) \cdot \vec{\sigma} \right] \vec{c}_{\vec{k}} \quad (2)$$

(cf. appendix A). In this expression for the Hamiltonian we introduced

$$\vec{c}_{\vec{k}} = \begin{pmatrix} c_{\vec{k}A} \\ c_{\vec{k}B} \end{pmatrix} \quad (3)$$

and the coefficient vector $\vec{d}_{\vec{k}}(t) = \left(d_{\vec{k}x}(t), d_{\vec{k}y}(t), d_{\vec{k}z}(t) \right)^T$ with

$$d_{\vec{k}x}(t) = -t_h \sum_{j=1}^3 \cos \left((\vec{k} - \vec{A}(t)) \cdot \vec{\delta}_j \right), \quad (4)$$

$$d_{\vec{k}y}(t) = -t_h \sum_{j=1}^3 \sin \left((\vec{k} - \vec{A}(t)) \cdot \vec{\delta}_j \right), \quad (5)$$

$$d_{\vec{k}z}(t) = 0 \quad (6)$$

as well as the vector of Pauli matrices $\vec{\sigma} = (\sigma^x, \sigma^y, \sigma^z)^T$. The vectors

$$\vec{\delta}_1 = \frac{a}{2} \begin{pmatrix} 1 \\ \sqrt{3} \end{pmatrix}, \quad \vec{\delta}_2 = \frac{a}{2} \begin{pmatrix} 1 \\ -\sqrt{3} \end{pmatrix}, \quad \vec{\delta}_3 = a \begin{pmatrix} -1 \\ 0 \end{pmatrix} \quad (7)$$

are given by the differences of the positions of neighboring lattice sites (cf. Fig. 2). Moreover,

$$\vec{A}(t) = \frac{V_0 a}{\omega} \begin{pmatrix} \sin(\omega t) \\ \cos(\omega t) \end{pmatrix}, \quad (8)$$

where a denotes the lattice spacing. In the following we will use the dimensionless driving amplitude $A = |\vec{A}(t)| = V_0 a \omega^{-1}$ to quantify the driving strength and, moreover, set $a \equiv 1$.

B. Periodic driving and Floquet formalism

In this section we recapitulate the Floquet formalism for the treatment of time-periodic Hamiltonians and thereby introduce the notation for the subsequent discussion. We closely follow the presentation and notation of Refs. [22, 23].

1. Effective Hamiltonian and micromotion operator

For a time-periodic Hamiltonian $H(t+T) = H(t)$ acting on a Hilbert space \mathcal{H} the Floquet theorem states that the Schrödinger equation

$$i \frac{d}{dt} |\psi(t)\rangle = H(t) |\psi(t)\rangle \quad (9)$$

is solved by *Floquet states* of the form

$$|\psi_n(t)\rangle = e^{-i\epsilon_n t} |\phi_n(t)\rangle \quad (10)$$

with *quasi-energies* ϵ_n and periodic *Floquet modes* $|\phi_n(t+T)\rangle = |\phi_n(t)\rangle$ [24, 25]. Note that ϵ_n and $|\phi_n(t)\rangle$ are not defined uniquely. Instead, given a solution ϵ_n and $|\phi_n(t)\rangle$, alternative choices are given by $\epsilon_{nm} = \epsilon_n + m\omega$ and $|\phi_{nm}(t)\rangle = e^{im\omega t} |\phi_n(t)\rangle$ with $\omega = 2\pi/T$ and $m \in \mathbb{Z}$, resulting in the same Floquet state

$$|\psi_n(t)\rangle = e^{-i\epsilon_n t} |\phi_n(t)\rangle = e^{-i\epsilon_{nm} t} |\phi_{nm}(t)\rangle. \quad (11)$$

Plugging eq. (11) into the Schrödinger equation (9) yields the Floquet equation

$$\left(H(t) - i \frac{d}{dt} \right) |\phi_{nm}(t)\rangle = \epsilon_{nm} |\phi_{nm}(t)\rangle, \quad (12)$$

which determines the Floquet modes and quasi-energies.

The Floquet states are eigenstates of the time evolution operator over one period, i.e.

$$U(t_0 + T, t_0) |\psi_n(t_0)\rangle = e^{-i\epsilon_n T} |\psi_n(t_0)\rangle, \quad (13)$$

and can therefore be regarded as eigenstates of a *Floquet Hamiltonian* $H_{t_0}^F$ defined by

$$U(t_0 + nT, t_0) = e^{-iH_{t_0}^F nT}. \quad (14)$$

The parameter t_0 is an arbitrary gauge choice for the Hamiltonian with the property that $H_{t_0+T}^F = H_{t_0}^F$. Introducing the corresponding gauge-dependent fast-motion operator

$$U_{t_0}^F(t) \equiv U(t, t_0) e^{iH_{t_0}^F(t-t_0)}, \quad (15)$$

which is time-periodic, $U_{t_0}^F(t+T) = U_{t_0}^F(t)$, the full time evolution operator can be expressed as

$$U(t_2, t_1) = U_{t_0}^F(t_2) e^{-iH_{t_0}^F(t_2-t_1)} U_{t_0}^F(t_1)^\dagger. \quad (16)$$

Since the quasi-energies ϵ_{nm} have no t_0 -dependence, the family of Floquet Hamiltonians, $H_{t_0}^F$, is moreover gauge equivalent to an *effective Hamiltonian* H_F , which has no explicit dependence on the driving phase t_0 [26]. The corresponding gauge transformation is determined by a Hermitian *kick operator* $\mathcal{K}(t)$ such that

$$H_F = e^{i\mathcal{K}(t_0)} H_{t_0}^F e^{-i\mathcal{K}(t_0)}. \quad (17)$$

Note that in general H_F alone does not generate the dynamics over one period. Nevertheless, the time evolution operator is still split as

$$U(t_2, t_1) = U_F(t_2) e^{-iH_F(t_2-t_1)} U_F(t_1)^\dagger, \quad (18)$$

where the *micromotion operator*

$$U_F(t) = e^{-i\mathcal{K}(t)} = U_F(t+T) \quad (19)$$

was introduced, and the eigenvalue problem

$$H_F |u_{nm}\rangle = \epsilon_{nm} |u_{nm}\rangle \quad (20)$$

determines the Floquet modes

$$|\phi_{nm}(t)\rangle = e^{im\omega t} U_F(t) |u_{nm}\rangle. \quad (21)$$

2. High frequency expansion of the effective Hamiltonian

Since they are periodic in time it is beneficial to view the Floquet modes $|\phi_{nm}(t)\rangle$ as elements of the composed *Sambe space* $\mathcal{S} = \mathcal{H} \otimes \mathcal{L}_T$, where \mathcal{L}_T is the space of T -periodic square integrable functions [27]. Given $\{|\alpha\rangle\}$ is a basis of \mathcal{H} , the vectors

$$|\alpha m\rangle\rangle = e^{im\omega t} |\alpha\rangle \quad (22)$$

constitute a basis of \mathcal{S} . Here we introduced the notation $|\cdot\rangle\rangle$ for vectors which are explicitly considered as elements of \mathcal{S} . With the natural scalar product in Sambe space we obtain

$$\begin{aligned} \langle\langle \alpha m | \alpha' m' \rangle\rangle &= \langle \alpha | \alpha' \rangle \frac{1}{T} \int_0^T dt e^{-i\omega(m-m')t} \\ &= \delta_{\alpha\alpha'} \delta_{mm'}. \end{aligned} \quad (23)$$

In these terms the operator

$$Q = H(t) - i \frac{d}{dt} \quad (24)$$

acts on \mathcal{S} and eq. (12) is an eigenvalue problem

$$Q|\phi_{nm}\rangle\rangle = \epsilon_{nm}|\phi_{nm}\rangle\rangle. \quad (25)$$

The matrix elements of Q are

$$\langle\langle\alpha'm'|Q|\alpha m\rangle\rangle = \langle\alpha'|H_{m'-m}|\alpha\rangle + \delta_{m'm}\delta_{\alpha'\alpha}m\omega \quad (26)$$

with the Fourier components of $H(t)$,

$$H_m = \frac{1}{T} \int_0^T dt e^{-im\omega t} H(t). \quad (27)$$

Eq. (26) reveals the block structure of Q with block indices m, m' . Eckardt and Anisimovas [22] identified the micromotion operator (19) as the operator, which block-diagonalizes (26), thereby yielding the time-independent effective Hamiltonian

$$H_F = U_F^\dagger(t)H(t)U_F(t) - iU_F^\dagger(t)\frac{d}{dt}U_F(t). \quad (28)$$

Making use of the large separation of diagonal matrix elements for large frequencies ω in eq. (26) they apply degenerate perturbation theory to derive expansions for the effective Hamiltonian as well as the micromotion operator in powers of $1/\omega$. As a result they find a way to express the effective Hamiltonian as a series

$$H_F = \sum_{n=0}^{\infty} \frac{1}{\omega^n} H_F^{(n)}, \quad (29)$$

which can be used to systematically approximate H_F at high frequencies. The same holds for the kick-operator, which takes the form

$$\mathcal{K}(t) = \sum_{n=1}^{\infty} \frac{1}{\omega^n} \mathcal{K}^{(n)}(t). \quad (30)$$

In our analysis we consider contributions to these series up to first order, which are

$$H_F^{(0)} = H_0, \quad H_F^{(1)} = \sum_{m=1}^{\infty} \frac{[H_m, H_{-m}]}{m} \quad (31)$$

and

$$\mathcal{K}^{(1)}(t) = -i \sum_{m=1}^{\infty} \frac{e^{im\omega t} H_m - e^{-im\omega t} H_{-m}}{m}. \quad (32)$$

C. Non-equilibrium Hall conductance

In the following we will study the Hall conductance of the stationary state that is reached after a quench of the driving amplitude at time t^* . We assume the system is prepared in an initial state $|\psi_0(t)\rangle\rangle$, which is the ground state of the Hamiltonian with driving amplitude $A_0 = 0$ or a quasi-stationary Floquet mode of the driven Hamiltonian with $A_0 \neq 0$. At time t_0 the driving amplitude is suddenly switched from A_0 to A_1 and a non-trivial time evolution is induced. We study the Hall conductance of the state the system reaches a long time after the quench. Based on linear response theory and using a dephasing argument Dehghani et al. [10] derived the following expression for the Hall conductance of a periodically driven electronic two-band system for this protocol obtaining

$$\sigma_{xy} = \frac{e^2}{2\pi\hbar} \int_{BZ} d^2k \bar{F}_{\bar{k}d} (\rho_{\bar{k}d}^-(t^*) - \rho_{\bar{k}u}^-(t^*)) \quad (33)$$

with the time-averaged Berry curvature

$$\bar{F}_{\bar{k}d} = \frac{2}{T} \int_0^T dt \text{Im} [\langle \partial_{k_y} \phi_{\bar{k}d}(t) | \partial_{k_x} \phi_{\bar{k}d}(t) \rangle] \quad (34)$$

and the occupation numbers of the Floquet modes,

$$\rho_{\bar{k}\alpha}^-(t^*) = |\langle \psi_0(t^*) | \phi_{\bar{k}\alpha}^-(t^*) \rangle|^2. \quad (35)$$

Here we introduced the indices $\alpha = u, d$ labeling the upper/lower band. In a cold atom setup with neutral atoms the electron charge e would be replaced by unity.

Dehghani et al. [10] considered quenches from the undriven ground state of the graphene Hamiltonian (2) to

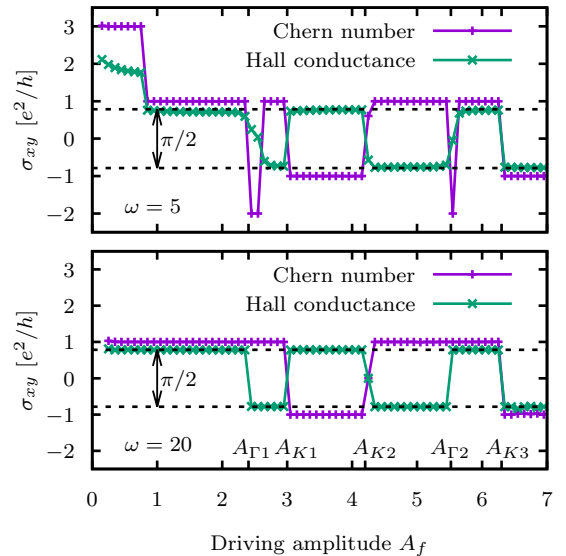


FIG. 3. Numerical results for the non-equilibrium Hall conductance after suddenly switching on the driving with amplitude A_f with the ground state of the undriven system as initial state for $\omega = 5$ (top) and $\omega = 20$ (bottom). The Chern number is computed according to eq. (36).

non-zero driving amplitudes A . They demonstrated that the Hall conductance as a function of the final driving amplitude changes rapidly whenever the Chern number

$$C = \frac{1}{2\pi} \int_{BZ} d^2k \bar{F}_{\vec{k}d} \quad (36)$$

jumps. We reproduced these numerical results as shown in Fig. 1a and Fig. 3 using the method described in appendix B of this paper.

Our results presented in section III provide an analytical understanding of the behavior of the non-equilibrium Hall conductance occurring under this protocol when quenching close to the transition points.

D. Non-analytic behavior of the Hall conductance of the quenched state for closed systems

For the case of closed systems Wang et al. [15, 16] studied an analogous situation to the one described above, considering quenches of a parameter M that allows to tune the Hamiltonian $H(M)$ between different topological phases. In a closed two-band system the Hall conductance of the stationary state after a quench is

$$\sigma_{xy} = \frac{e^2}{\pi h} \int_{BZ} d^2k \text{Im} [\langle \partial_{k_y} \varphi_{\vec{k}d} | \partial_{k_x} \varphi_{\vec{k}d} \rangle] (\rho_{\vec{k}d} - \rho_{\vec{k}u}) , \quad (37)$$

where $|\varphi_{\vec{k}\alpha}\rangle$ are the eigenstates of the post-quench Hamiltonian $H(M_f)$ and $\rho_{\vec{k}\alpha} = |\langle \psi_0 | \varphi_{\vec{k}\alpha} \rangle|^2$ are the occupation numbers of these eigenstates after the quench. The expressions for the Hall conductance in eq. (33) and eq. (37) have very similar structure and, in fact, also in the case of the closed system the Hall conductance of the quenched state changes significantly when the quench parameter approaches an equilibrium phase boundary. In particular, considering the non-equilibrium Hall conductance close to a phase boundary M_c one finds that the behavior close to critical points is dominated by the non-analytic part

$$\sigma_{xy}^{\text{div.}} = \frac{e^2}{h} \sum_{\vec{q}} \mathcal{C}_{\eta}^{(\vec{q})}(M_i, M_f) \quad (38)$$

with

$$\mathcal{C}_{\eta}^{(\vec{q}_j)} = \int_{\mathcal{B}_{\eta}(\vec{q}_j)} \frac{d^2k}{\pi} \text{Im} [\langle \partial_{k_y} \varphi_{\vec{k}d} | \partial_{k_x} \varphi_{\vec{k}d} \rangle] (\rho_{\vec{k}d} - \rho_{\vec{k}u}) , \quad (39)$$

where $\mathcal{B}_{\eta}(\vec{q}_j)$ is a circle of radius η centered at \vec{q}_j , the gap-closing points of the quasi-energy spectrum in the Brillouin zone. If the parameter $M - M_c$ is chosen proportional to the gap size the derivative of these contributions diverges as

$$\frac{d\sigma_{xy}^{\text{div.}}}{dM_f} \sim \frac{e^2}{h} \frac{C_f^- - C_f^+}{2|M_i - M_c|} \ln |M_f - M_c| , \quad (40)$$

where C_f^{\pm} are the Chern numbers on the right hand side (+, $M_f > M_c$) and left hand side (-) of the transition, respectively. This constitutes a universal non-analytic behavior of the non-equilibrium Hall conductance σ_{xy} . The result above is obtained by expanding the coefficient vector $\vec{d}_{\vec{k}}$, which is for any two-band system defined analogously to eq. (2), around the gap closing points \vec{q} ,

$$\vec{d}_{\vec{k}} = \vec{d}_{\vec{q}} + \hat{J}_{\vec{q}}^{\vec{d}} \Delta \vec{k} + \mathcal{O}(\Delta \vec{k}^2) , \quad (41)$$

where $\hat{J}_{\vec{q}}^{\vec{d}}$ is the Jacobian matrix of $\vec{d}_{\vec{k}}$. The integral over the Brillouin zone in eq. (37) is for M_f close to M_c dominated by contributions from the vicinity of gap closing points. The remaining part $\sigma_{xy} - \sigma_{xy}^{\text{div.}}$ is an analytic function which is in particular continuous. Any non-analyticity of the Hall conductance is contributed by $\sigma_{xy}^{\text{div.}}$. Note that the terms of $\mathcal{O}(\Delta \vec{k}^2)$ do not contribute to the non-analytic behavior, as discussed in Ref. [16]. The non-analyticity can therefore be analyzed based on the expansion to linear order in eq. (41) yielding the result in eq. (40).

Note that, remarkably, the Dirac cones also lead to universal behavior of the Hall conductance away from the critical points as shown in Ref. [28].

In the following we will extend this analysis to the case of driven systems based on a high frequency expansion of the effective Hamiltonian and the micromotion operator.

III. RESULTS

A. Time-averaged Berry curvature and Berry connection

An important property of the Berry curvature $\Omega_{\vec{k}}$ in undriven systems is the fact that it can be related to a local gauge potential, namely the Berry connection $\vec{A}_{\vec{k}}$, via

$$\Omega_{\vec{k}} = \vec{\nabla} \times \vec{A}_{\vec{k}} . \quad (42)$$

This property implies through the Kelvin-Stokes theorem that the Chern number is an integer [29].

It should be noted that it is a priori not clear whether a corresponding time-averaged Berry connection can be attributed to the time-averaged Berry curvature $\bar{F}_{\vec{k}d}$ defined in eq. (34), because for a non-vanishing Chern number the Berry connection must exhibit singularities, which could prohibit exchanging integrals and derivatives unheedingly. Nevertheless, we argue in this section that the time-averaged Berry curvature is at least up to corrections of second order in ω^{-1} given by the Berry curvature of the effective Hamiltonian, which is related to a Berry connection.

Applying the product rule for the derivatives the time-averaged Berry curvature (34) can be split into two parts

when plugging in eq. (21) for the Floquet modes, yielding

$$\begin{aligned} \bar{F}_{\vec{k}d} &= \Omega_{\vec{k}}^F \\ &+ \frac{2}{T} \int_0^T dt \operatorname{Im} \left[\langle u_{\vec{k}}^d | (\partial_{k_y} U_F(t)^\dagger) U_F(t) | \partial_{k_x} u_{\vec{k}}^d \rangle \right. \\ &\quad + \langle \partial_{k_y} u_{\vec{k}}^d | U_F(t)^\dagger (\partial_{k_x} U_F(t)) | u_{\vec{k}}^d \rangle \\ &\quad \left. + \langle u_{\vec{k}}^d | (\partial_{k_y} U_F(t)^\dagger) (\partial_{k_x} U_F(t)) | u_{\vec{k}}^d \rangle \right] \quad (43) \end{aligned}$$

with $\Omega_{\vec{k}}^F = 2 \operatorname{Im}[\langle \partial_{k_y} u_{\vec{k}}^d | \partial_{k_x} u_{\vec{k}}^d \rangle]$ the Berry curvature of the effective Hamiltonian H_F . For the derivatives of the operator exponentials $U_F(t) = \exp(-i\mathcal{K}(t))$ we employ the identity

$$\frac{d}{d\lambda} e^{-i\mathcal{K}(t)} = \int_0^1 ds e^{-(1-s)i\mathcal{K}(t)} \frac{d\mathcal{K}(t)}{d\lambda} e^{-si\mathcal{K}(t)} \quad (44)$$

given in Ref. [30]. This reveals that the last term in eq. (43) is of $\mathcal{O}(\omega^{-2})$, because $\mathcal{K}(t) \sim \mathcal{O}(\omega^{-1})$. For the remaining terms the Baker-Campbell-Hausdorff formula yields

$$\begin{aligned} (\partial_{k_y} U_F(t)^\dagger) U_F(t) &= \int_0^1 ds e^{i(1-s)\mathcal{K}(t)} \frac{\partial \mathcal{K}(t)}{\partial k_y} e^{-i(1-s)\mathcal{K}(t)} \\ &= \frac{d\mathcal{K}(t)}{dk_y} + \frac{i}{2} [\mathcal{K}(t), \partial_{k_y} \mathcal{K}(t)] + \dots \\ &= \frac{d\mathcal{K}(t)}{dk_y} + \mathcal{O}(\omega^{-2}) \quad (45) \end{aligned}$$

The ellipsis after the second equality stands for higher nested commutators with $\mathcal{K}(t)$, which are all of higher order in ω^{-1} . The analogous argument yields $U_F(t)^\dagger (\partial_{k_x} U_F(t)) = \frac{d\mathcal{K}(t)}{dk_x} + \mathcal{O}(\omega^{-2})$. Now, according to eq. (32), the time dependence of the first order contribution to the kick operator, $\mathcal{K}^{(1)}(t)$, is given as a sum of $e^{im\omega t}$ with $m \neq 0$. Hence, $\int_0^T dt \partial_{k_x/y} \mathcal{K}^{(1)}(t) = 0$ and we obtain

$$\bar{F}_{\vec{k}d} = \Omega_{\vec{k}}^F + \mathcal{O}(\omega^{-2}). \quad (46)$$

Note moreover, that if despite the singularities in $\bar{F}_{\vec{k}d}$ the time integral and derivatives with respect to \vec{k} can be exchanged the time-averaged Berry curvature can be written as the curl of a time-averaged Berry connection

$$\bar{A}_{\vec{k}d}^\alpha = \frac{1}{T} \int_0^T dt \langle \phi_{\vec{k}d}(t) | \partial_{k_\alpha} | \phi_{\vec{k}d}(t) \rangle \quad (47)$$

meaning that due to the usual arguments the Chern number $C = \frac{1}{2\pi} \int_{BZ} d^2 k \vec{\nabla} \times \bar{A}_{\vec{k}d}$ is an integer. That is, however, only possible if all higher order terms in eq. (46) vanish and C is identically the Chern number of the effective Hamiltonian H_F .

B. High frequency expansion

For the subsequent analysis it is useful to formulate both the high frequency expansion of the effective Hamiltonian and the expansion of the kick operator in terms

of coefficient vectors $\vec{h}_{\vec{k}}$ and $\vec{g}_{\vec{k}}(t)$ such that in the single momentum sectors

$$H_{\vec{k}F} = \vec{h}_{\vec{k}} \cdot \vec{\sigma} \quad (48)$$

and

$$\mathcal{K}_{\vec{k}}(t) = -\vec{g}_{\vec{k}}(t) \cdot \vec{\sigma}. \quad (49)$$

In this section we present expressions for the time averaged Berry curvature and the Floquet mode occupation based on expansions of the respective coefficient vectors.

We will from now on set the hopping $t_h \equiv 1$. This means that the high frequency expansion is valid for $\omega/t_h = \omega \gg 1$.

1. Effective Hamiltonian and Berry curvature

For the high frequency expansion of the effective Hamiltonian given in eq. (31) we need the Fourier components of the time-dependent Hamiltonian $H_{\vec{k}}(t) = \vec{d}_{\vec{k}}(t) \cdot \vec{\sigma}$. These are determined by

$$\begin{aligned} d_{\vec{k}x}^m &= \frac{1}{T} \int_0^T dt e^{im\omega t} d_{\vec{k}x}(t) \\ &= -J_m(A) \sum_{j=1}^3 \frac{1}{2} e^{-im\psi_j} \left[e^{i\vec{k} \cdot \vec{\delta}_j} + (-1)^m e^{-i\vec{k} \cdot \vec{\delta}_j} \right] \\ d_{\vec{k}y}^m &= -J_m(A) \sum_{j=1}^3 \frac{-i}{2} e^{-im\psi_j} \left[e^{i\vec{k} \cdot \vec{\delta}_j} + (-1)^{m+1} e^{-i\vec{k} \cdot \vec{\delta}_j} \right], \quad (50) \end{aligned}$$

where $J_m(x)$ denotes the m -th Bessel function and $\psi_j = \arctan(\delta_j^y/\delta_j^x)$ was introduced. This yields as the zeroth order term of the effective Hamiltonian just the undriven Hamiltonian rescaled by the zeroth Bessel function,

$$\vec{h}_{\vec{k}}^{(0)}(A) = -J_0(A) \sum_{j=1}^3 \begin{pmatrix} \cos(\vec{k} \cdot \vec{\delta}_j) \\ \sin(\vec{k} \cdot \vec{\delta}_j) \\ 0 \end{pmatrix}. \quad (51)$$

As the first order term is the commutator of only the Pauli matrices σ_x and σ_y there is only a contribution to the z -component of the coefficient vector, namely

$$h_{\vec{k}z}^{(1)}(A) = 4 \sum_{n=1}^{\infty} \frac{J_n(A)^2 \sin\left(\frac{2n\pi}{3}\right)}{n} \sum_{j=1}^3 \sin(\vec{k} \cdot \vec{\gamma}_j), \quad (52)$$

where the next-nearest-neighbor vectors

$$\vec{\gamma}_1 = \vec{\delta}_1 - \vec{\delta}_3, \quad \vec{\gamma}_2 = \vec{\delta}_2 - \vec{\delta}_1, \quad \vec{\gamma}_3 = \vec{\delta}_3 - \vec{\delta}_2 \quad (53)$$

were introduced. Note that since $J_n(A)^2/n$ decreases with increasing n the infinite sum in eq. (52) can for practical purposes safely be approximated by a truncation restricted to the first few terms. Fig. 4 shows the

analytical result for $h_{\vec{q}_z}^{(1)}(A)$ for $\omega = 10$ in comparison with the numerical result at the Dirac points (K -points)

$$\vec{q}_{\pm} = \begin{pmatrix} 0 \\ \pm \frac{4\pi}{3\sqrt{3}a} \end{pmatrix}. \quad (54)$$

Both show good agreement, in particular in the vicinity of the roots.

The appearance of the n.n.n.-vectors in the effective Hamiltonian reflects the fact that in real space the first order contribution to the effective Hamiltonian adds a hopping between next-nearest neighbors. The resulting effective Hamiltonian corresponds to the famous Haldane model where in this case the external driving opens a gap in the quasi-energy spectrum leading to a non-vanishing Chern number [3, 7, 22].

Omitting possible second order contributions to the time-averaged Berry curvature as discussed in section III A the Chern number (36) is solely determined by the effective Hamiltonian H_F and can be expressed in terms of the coefficient vector $\vec{h}_{\vec{k}}$ as

$$C = \int_{BZ} d^2k \frac{\left(\frac{\partial \vec{h}_{\vec{k}}}{\partial k_x} \times \frac{\partial \vec{h}_{\vec{k}}}{\partial k_y} \right) \cdot \vec{h}_{\vec{k}}}{4\pi(h_{\vec{k}})^3} \quad (55)$$

(cf. [29]).

Note that there are different possibilities for gap closing points in the quasi-energy spectrum of the effective Hamiltonian, which reads to first order

$$H_{F\vec{k}} = h_{\vec{k}x}^{(0)} \sigma^x + h_{\vec{k}y}^{(0)} \sigma^y + \frac{1}{\omega} h_{\vec{k}z}^{(1)} \sigma^z + \mathcal{O}(\omega^{-2}). \quad (56)$$

Independent of the driving amplitude the zeroth-order terms have roots at the Dirac points \vec{q}_{\pm} . Therefore, roots of $h_{\vec{q}_{\pm z}}^{(1)}(A)$ as function of the driving amplitude mark gap-closing points. Moreover, $h_{\vec{k}z}^{(1)}(A)$ has a root at the Γ -point $\vec{k}_{\Gamma} = (0,0)$ independent of driving amplitude. This means that the quasi-energy spectrum closes at this point at roots of $J_0(A)$, because there the zeroth order terms vanish on the whole Brillouin zone. We marked the transitions that can be attributed to gap closing points at K or Γ points with labels A_{K_i} and A_{Γ_i} , respectively, in Fig. 3. In the following analysis we will focus on the transitions with gap closing at the K -points.

2. Micromotion operator and occupation numbers

The second ingredient for the Hall conductance of the quenched state is the mode occupation difference

$$\begin{aligned} \rho_{\vec{k}d}(t^*) - \rho_{\vec{k}u}(t^*) \\ = |\langle \psi_0(t^*) | \phi_{\vec{k}d}(t^*) \rangle|^2 - |\langle \psi_0(t^*) | \phi_{\vec{k}u}(t^*) \rangle|^2, \end{aligned} \quad (57)$$

which depends on the quench time t^* . Fig. 5a shows the mode occupation in the Brillouin zone for a quench

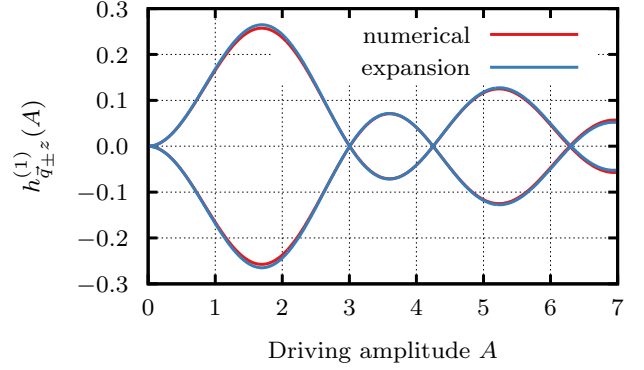


FIG. 4. Values of the first order contribution to the z -component of the coefficient vector at the Dirac points, $h_{\vec{q}_{\pm z}}^{(1)}(A)/\omega$, for $\omega = 10$ as function of the driving amplitude A in comparison with the numerical result for $h_{\vec{q}_{\pm z}}(A)$.

from $A_0 = 0.1$ to $A_1 = 2.8$ at $t_0 = 0$. Quenching the amplitude leads to a smearing of the occupation numbers along the direction of the driving field. Since we consider quasi-stationary Floquet modes as initial states, the time dependence is fully determined by the pre- and post-quench micromotion operators.

As given by eq. (32) the first order term of the high frequency expansion of the kick operator is

$$\mathcal{K}_{\vec{k}}^{(1)}(t) = -i \sum_{m=1}^{\infty} \frac{1}{m} \left[e^{im\omega t} \vec{d}_{\vec{k}}^m - e^{-im\omega t} \vec{d}_{\vec{k}}^m \right] \cdot \vec{\sigma} \quad (58)$$

with $\vec{d}_{\vec{k}}^m$ given in eq. (50). We approximate the micromotion operator with

$$U_{\vec{k}}^F(t) = \exp \left(-i \mathcal{K}_{\vec{k}}^{(1)}(t)/\omega \right) + \mathcal{O}(\omega^{-2}) \quad (59)$$

and define $\vec{g}_{\vec{k}}(t) = (g_{\vec{k}x}(t), g_{\vec{k}y}(t), g_{\vec{k}z}(t))$ via

$$-\mathcal{K}_{\vec{k}}^{(1)}(t) = \vec{g}_{\vec{k}}(t) \cdot \vec{\sigma}. \quad (60)$$

This approximation of the micromotion operator and the first order result for the eigenvectors of the effective Hamiltonian yields via eq. (21) the t_0 -dependent occupation numbers

$$\begin{aligned} \rho_{\vec{k}d}(t^*) - \rho_{\vec{k}u}(t^*) \\ = \frac{\vec{h}_{\vec{k}}^i \cdot \vec{h}_{\vec{k}}^f}{|h_{\vec{k}}^i| |h_{\vec{k}}^f|} + \frac{\left(\vec{h}_{\vec{k}}^i \times \vec{h}_{\vec{k}}^f \right) \cdot \Delta \vec{g}(t^*)}{|h_{\vec{k}}^f| |h_{\vec{k}}^i|} + \mathcal{O}(\omega^{-2}). \end{aligned} \quad (61)$$

Here $\Delta \vec{g}_{\vec{k}}(t^*) = \vec{g}_{\vec{k}}^{A_f}(t^*) - \vec{g}_{\vec{k}}^{A_i}(t^*)$ denotes the difference of the Kick operator coefficients before and after switching the driving amplitude. A detailed derivation of this result is given in appendix C.

Fig. 5b shows a comparison between the analytical result in eq. (61) and the numerical result on cuts through

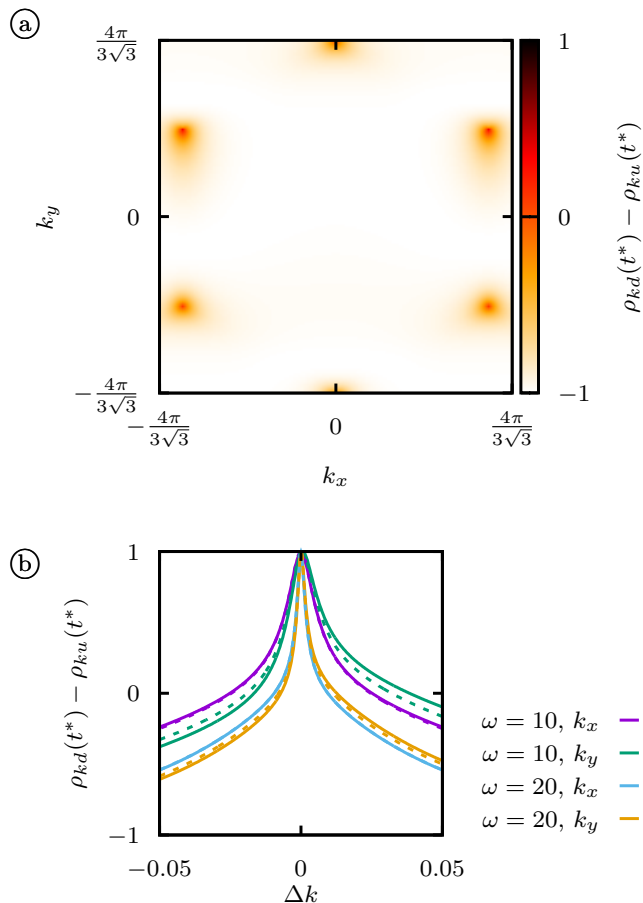


FIG. 5. a – Numerical result for the mode occupation after quenching the driving amplitude from $A_0 = 0.1$ to $A_1 = 2.8$ at $t^* = 0$. b – Comparison between numerical results (solid lines) and the high frequency expansion (61) (dashed lines) along cuts with constant k_x or k_y , respectively, through the K -point $\vec{q} = (0, -4\pi/3\sqrt{3})$ for two different frequencies.

a K -point with constant k_x and k_y , respectively, for two different driving frequencies. The truncated high frequency expansion clearly captures the anisotropy introduced by the external field and the agreement with numerics improves as the driving frequency is increased.

In order to analyze the non-analytic part of the Hall conductance (39) it is crucial that the occupation numbers contribute a factor $|h_{\vec{k}}^f|^{-1}$, because thereby the denominator becomes a polynomial and it is possible to find the antiderivative of the integrand. The result in eq. (61) shows that the correction is proportional to $|h_{\vec{k}}^f|^{-1}$. Moreover, the first order contribution to the occupation numbers is an odd function of $\Delta\vec{k} = \vec{k} - \vec{q}_{\pm}$. Therefore, as discussed in Ref. [16], the corresponding part of the integrand will not contribute to the non-analytic behavior of the Hall conductance (34). This means that close to the phase boundaries any dependence of the Hall conductance on the quench time is a second order contribution in powers of the inverse frequency. We will therefore ig-

nore it in the further analysis.

Experimental setups with finite ramping times will usually not be able to prepare initial states with a completely filled lower band and an empty upper band. Nevertheless, we will focus on this situation in the following analysis and discuss the effect of partially filled bands as initial states later in section III D.

C. Universal behavior at the phase transition

Putting together eqs. (34), (46), and (61) the non-equilibrium Hall conductance is determined by

$$\sigma_{xy} = \frac{e^2}{h} \int d\vec{k}^2 \frac{(\vec{h}_{\vec{k}}^f \cdot \vec{h}_{\vec{k}}^i) \left(\frac{\partial \vec{h}_{\vec{k}}^f}{\partial k_x} \times \frac{\partial \vec{h}_{\vec{k}}^f}{\partial k_y} \right) \cdot \vec{h}_{\vec{k}}^f}{4\pi h_{\vec{k}}^i (h_{\vec{k}}^f)^4} \quad (62)$$

where the integral is over the Brillouin zone.

We will analyze the non-analytic behavior of (62) based on expansions of the integrand around the gap closing points as summarized in section II D and discussed more extensively in Ref. [16]. According to the high frequency expansion to first order in powers of ω^{-1} , we can suppose the coefficient vectors $\vec{h}_{\vec{k}}^{i/f}$ of the initial and final Hamiltonian, respectively, around some singularity \vec{q} to be

$$h_{\vec{k}x}^{i/f} = J_0(A_{i/f}) (a_{1x}\Delta k_x + a_{1y}\Delta k_y) + \mathcal{O}(\Delta k^2) \quad (63)$$

$$h_{\vec{k}y}^{i/f} = J_0(A_{i/f}) (a_{2x}\Delta k_x + a_{2y}\Delta k_y) + \mathcal{O}(\Delta k^2) \quad (64)$$

$$h_{\vec{k}z}^{i/f} = m(A_{i/f}) + \mathcal{O}(\Delta k^2), \quad (65)$$

where $\Delta k_{x/y} = k_{x/y} - q_{x/y}$. Note that A_i and A_f are the free parameters and $m(A_{i/f}) = h_{\vec{q}z}^{(1)}(A_{i/f})$ is also a function of $A_{i/f}$. In contrast to the closed system analyzed in Refs. [15, 16] for the driven system the expansion coefficients of all components depend on the external parameter, namely the driving amplitude A . However, by introducing the expansion

$$h_{\vec{k}x}^{*i/f} = a_{1x}\Delta k_x + a_{1y}\Delta k_y + \mathcal{O}(\Delta k^2) \quad (66)$$

$$h_{\vec{k}y}^{*i/f} = a_{2x}\Delta k_x + a_{2y}\Delta k_y + \mathcal{O}(\Delta k^2) \quad (67)$$

$$h_{\vec{k}z}^{*i/f} = \frac{m(A_{i/f})}{J_0(A_{i/f})} + \mathcal{O}(\Delta k^2) \equiv \tilde{m}_{i/f} + \mathcal{O}(\Delta k^2). \quad (68)$$

the structure of the integrand in eq. (62) remains the same and we obtain the non-analytic contributions defined in eq. (39), which read

$$\mathcal{C}_{\eta}^{(\vec{q})} = \text{sgn}(J_0(A_i)) \times \int_{\mathcal{B}_{\eta}(\vec{q}_j)} d\vec{k}^2 \frac{(\vec{h}_{\vec{k}}^{*f} \cdot \vec{h}_{\vec{k}}^{*i}) \left(\frac{\partial \vec{h}_{\vec{k}}^{*f}}{\partial k_x} \times \frac{\partial \vec{h}_{\vec{k}}^{*f}}{\partial k_y} \right) \cdot \vec{h}_{\vec{k}}^{*f}}{4\pi h_{\vec{k}}^{*i} (h_{\vec{k}}^{*f})^4}. \quad (69)$$

Therefore, the analysis of the behavior of the Hall conductance close to a transition can be done based on the expansion (66)-(68) with constant coefficients in the first two components given that $J_0(A_{i/f}) \neq 0$. As mentioned above, it is sufficient to consider the expansion to linear order. In the vicinity of roots of $J_0(A_{i/f})$, however, the corresponding expansions of the first two components of the coefficient vectors are potentially dominated by higher order contributions.

1. Quenching from the undriven initial state

We first focus on the quenches with the ground state of the undriven system as initial state, i.e. $A_i = 0$ and $A_f \neq 0$. The gaplessness of the initial Hamiltonian is reflected by $\tilde{m}_i = 0$ in eq. (68), whereas $\tilde{m}_f \neq 0$. The linear transformation of coordinates

$$\begin{pmatrix} \Delta k'_x \\ \Delta k'_y \end{pmatrix} = \begin{pmatrix} a_{1x} & a_{1y} \\ a_{2x} & a_{2y} \end{pmatrix} \begin{pmatrix} \Delta k_x \\ \Delta k_y \end{pmatrix} \quad (70)$$

allows to make use of the rotational symmetry around the singularity, yielding

$$\begin{aligned} \mathcal{C}_\eta^{(\bar{q})} &= \mathbf{sgn}(J_0(A_i)) \frac{\tilde{m}_f \mathbf{sgn}(a_{1x}a_{2y} - a_{2x}a_{1y})}{2} \\ &\times \int_0^\eta d\Delta k' \frac{\Delta k'^2}{(\tilde{m}_f^2 + \Delta k'^2)^2}. \end{aligned} \quad (71)$$

The non-vanishing part of this integral in the limit $m_f \rightarrow 0$ is

$$\begin{aligned} &\frac{\tilde{m}_f \mathbf{sgn}(a_{1x}a_{2y} - a_{2x}a_{1y})}{4} \int_0^\eta d\Delta k' \frac{1}{\tilde{m}_f^2 + \Delta k'^2}. \quad (72) \\ &= \frac{\mathbf{sgn}(a_{1x}a_{2y} - a_{2x}a_{1y})}{4} \arctan(\eta/\tilde{m}_f). \end{aligned} \quad (73)$$

For arbitrary $\eta > 0$, we have $\lim_{m_f \rightarrow 0} \arctan(\eta/\tilde{m}_f) = \mathbf{sgn}(\tilde{m}_f)\pi/2$. Thus, the discontinuity of $\mathcal{C}_\eta^{(\bar{q})}$ at $m_f = 0$ must be

$$\begin{aligned} &\mathcal{C}_\eta^{(\bar{q})}(m_f \rightarrow 0^+) - \mathcal{C}_\eta^{(\bar{q})}(m_f \rightarrow 0^-) \\ &= \frac{\pi}{4} \mathbf{sgn}[J_0(A_i)J_0(A_f)(a_{1x}a_{2y} - a_{2x}a_{1y})]. \end{aligned} \quad (74)$$

Summing up the contributions of both K -points according to eq. (38) yields the discontinuity of the total Hall conductance, which is

$$\begin{aligned} &\sigma_{xy}(A_f - A_c \rightarrow 0^+) - \sigma_{xy}(A_f - A_c \rightarrow 0^-) \\ &= \frac{\pi}{4} \mathbf{sgn}\left(\frac{J_0(A_i)}{J_0(A_f)}\right) \left[\lim_{m_f \rightarrow 0^+} C - \lim_{m_f \rightarrow 0^-} C \right] \\ &= \pm \frac{\pi e^2}{2h}. \end{aligned} \quad (75)$$

The sign depends on the particular choice of the gap closing point A_c . For critical points which are related to a closing of the gap at the K -points in the Brillouin zone the comparison with the numerical results in Fig. 1a and Fig. 3 shows that the dimensionless Hall conductance indeed jumps by $\pi/2$.

2. Quenching from a driven initial state

We now turn to the case where the system is initially prepared in a quasi-stationary Floquet mode of the driven Hamiltonian with $A_i \neq 0$. When the initial state is a Floquet mode of the driven Hamiltonian, the analysis is completely analogous to the case of the closed system in Refs. [15, 16]. Plugging eqs. (66)-(68) into eq. (69) yields the non-analytic part of the integral, which is

$$\begin{aligned} \mathcal{C}_\eta^{(\bar{q})} &\sim -\frac{J_0(A_i)}{J_0(A_f)} \frac{\mathbf{sgn}(a_{1x}a_{2y} - a_{2x}a_{1y})}{2|m_i|} \\ &\times m_f(A_f) \ln \left| \frac{m_f(A_f)}{J_0(A_f)} \right|. \end{aligned} \quad (76)$$

Note first of all that by contrast to quenching from the undriven ground state the Hall conductance is continuous at the transition points if the initial state is a Floquet mode of the driven Hamiltonian, which is also evident in Fig. 1a. Nevertheless, the derivative with respect to A_f in the limit $A_f \rightarrow A_f^c$ is non-analytic and diverges like

$$\begin{aligned} \frac{d\mathcal{C}_\eta^{(\bar{q})}}{dA_f} &\sim -\frac{J_0(A_i)}{J_0(A_f^c)} \frac{\mathbf{sgn}(a_{1x}a_{2y} - a_{2x}a_{1y})}{2|m_i|} \\ &\times \left. \frac{dm_f}{dA_f} \right|_{A_f=A_f^c} \ln |m_f(A_f)|. \end{aligned} \quad (77)$$

Summing up the contributions from both gap closing points in the Brillouin zone yields the divergent part of the derivative of the Hall conductance

$$\begin{aligned} \frac{d\sigma_{xy}^{\text{div.}}}{dA_f} &\sim \frac{J_0(A_i)}{J_0(A_f^c)} \frac{\lim_{m_f \rightarrow 0^+} C - \lim_{m_f \rightarrow 0^-} C}{2|m_i|} \\ &\times \left. \frac{dm_f}{dA_f} \right|_{A_f=A_f^c} \ln |m_f(A_f)|. \end{aligned} \quad (78)$$

Fig. 1b shows the derivative of the Hall conductance for quenches with different A_i and A_f close to the transition K_1 . The derivatives have been rescaled by the respective prefactors $\mu(A_i, A_f) = J_0(A_f)|m_i|/J_0(A_i)m'_f$ such that according to eq. (77) the slopes of all results coincide. Moreover, the results for different A_i have been shifted by in order to compare them despite the different regular contributions to the Hall conductance. The numerical data agree with the analytically predicted slope and the agreement improves as A_f approaches the transition point A_{K1} . Note that after a quench starting with $A_i = 2.3$ the agreement is good although this is very close to a root of $J_0(A_i)$ as can be seen in the inset of Fig. 1b.

The presented data were obtained using a grid with 6000×6000 points in the numerical scheme described in appendix B. This grid resolution determines the computational cost and has to be increased as A_f approaches A_{K1} . Thereby our computational resources limit the numerical results to the regime presented in Fig. 1b.

D. The effect of partially filled Floquet bands as initial state

As mentioned before the completely filled lower Floquet band we considered above cannot necessarily be prepared with high fidelity in practice [9, 31]. In particular, ramping across a gap closing point prohibits adiabatic preparation of the initial state. Therefore, the initial state will typically be given by partially filled Floquet bands in experiments.

Considering partially filled bands produced using some ramping protocol the single particle initial states will be a

superposition of the pre-quench Floquet modes $|\phi_{0\vec{k}}^\alpha(t)\rangle$,

$$|\psi_{\vec{k}}^0(t)\rangle = \cos\theta_{\vec{k}}|\phi_{0\vec{k}}^d(t)\rangle + \sin\theta_{\vec{k}}e^{i\varphi_{\vec{k}}(t)}|\phi_{0\vec{k}}^u(t)\rangle. \quad (79)$$

In this expression $\theta_{\vec{k}}$ parametrizes the single particle occupation number and it will depend on the details of the ramping protocol. The phase is given by $\varphi_{\vec{k}}(t) = \varphi_{\vec{k}}^0 + (\epsilon_{\vec{k}}^d - \epsilon_{\vec{k}}^u)t = \varphi_{\vec{k}}^0 - 2|\vec{h}_{0\vec{k}}^i|t$, where $\vec{h}_{0\vec{k}}$ is the coefficient vector of the initial effective Hamiltonian. Plugging this into eq. (57) yields

$$\begin{aligned} \rho_{\vec{k}}^d(t^*) - \rho_{\vec{k}}^u(t^*) &= \cos(2\theta_{\vec{k}}) \left(|\langle \phi_{0\vec{k}}^d(t^*) | \phi_{\vec{k}}^d(t^*) \rangle|^2 - |\langle \phi_{0\vec{k}}^d(t^*) | \phi_{\vec{k}}^u(t^*) \rangle|^2 \right) \\ &+ \sin(2\theta_{\vec{k}}) \operatorname{Re} \left[e^{i\varphi_{\vec{k}}(t^*)} \left(\langle \phi_{0\vec{k}}^d(t^*) | \phi_{\vec{k}}^d(t^*) \rangle \langle \phi_{\vec{k}}^d(t^*) | \phi_{0\vec{k}}^u(t^*) \rangle - \langle \phi_{0\vec{k}}^d(t^*) | \phi_{\vec{k}}^u(t^*) \rangle \langle \phi_{\vec{k}}^u(t^*) | \phi_{0\vec{k}}^u(t^*) \rangle \right) \right] \end{aligned} \quad (80)$$

Thereby, the Hall conductance after a quench can be split into two parts, $\sigma_{xy} = \sigma_{xy}^{(1)} + \sigma_{xy}^{(2)}$, corresponding to the first and the second contribution to the occupation difference.

The first term of the occupation difference above equals the occupation difference one obtains when the system is initialized in the lower Floquet band weighted by the prefactor $\cos(2\theta_{\vec{k}})$. The specific form of the occupation after preparation, which is parametrized by $\theta_{\vec{k}}$, will depend on the preparation protocol. If $\theta_{\vec{k}}$ can be approximated by a constant in the vicinity of the gap closing points \vec{q}_j it will not affect the non-analytic behavior and $\sigma_{xy}^{(1)}$ will contribute a logarithmic divergence to the derivative of the Hall conductance at the critical time. In the case of the driven hexagonal system considered above the non-analyticity in eq. (77) acquires an additional prefactor $\cos(\theta_{\vec{q}})$ with \vec{q} given in eq. (54).

Under the assumption that both $\theta_{\vec{k}}$ and $\varphi_{\vec{k}}^0$ are well behaved in the vicinity of the gap closing points the second term yields a contribution to the non-equilibrium Hall conductance that is independent of the driving frequency and behaves like the Hall conductance after quenching from a critical state, as discussed in section III C 1, but is weighted with $\sin(\theta_{\vec{q}})$ and oscillates with frequency $2|\vec{h}_{\vec{q}}^i|$, i.e. the initial gap width. For our specific model and the class of critical points we considered above the contribution is

$$\pm \sin(2\theta_{\vec{k}_0}) \cos(\varphi_{\vec{k}_0}^0(t^*)) \frac{\pi e^2}{2h} \quad (81)$$

A detailed derivation of this result is given in appendix D. This contribution is non-universal as it depends on the quench time t^* . However, it can in practice be eliminated by averaging over a range of quench times t^* .

Altogether the results obtained for the completely filled lower Floquet band will pertain when allowing par-

tially filled Floquet bands as initial states if the occupation numbers in the vicinity of gap closing points are well behaved. Non-analyticities in the occupation difference, however, could potentially lead to different behavior of the non-equilibrium Hall conductance.

Any kind of occupation that reflects the spectral properties of a gapped system will be smooth in the vicinity of the gap closing points \vec{q} . For example, thermal occupation numbers corresponding to an inverse temperature β are obtained from the pure state (79) if $\cos\theta_{\vec{k}} = e^{-\beta\epsilon_{\vec{k}}^d/2} (2 \cosh(\beta\epsilon_{\vec{k}}^d))^{-1/2}$, where the (quasi-)energies $\epsilon_{\vec{k}}$ are smooth everywhere. Nevertheless, ramping across gap closing points could possibly leave an imprint of the non-analyticity in the resulting occupation numbers. Moreover, it might be possible that the characteristics of the occupation depend on the choice of the ramping protocol. Such effects, since beyond the scope of this work, should be investigated in the future.

IV. DISCUSSION

A. Universality

The non-analytic behavior of the Hall conductance at the critical points studied in this work is universal in the same sense as discussed in Ref. [16]. The key feature that determines the non-analytic behavior is the conic structure of the quasi-energy spectrum close to the gap closing point. Thereby, the non-analytic behavior does not depend on the details of the model.

Both expressions characterizing the non-analytic behavior, eq. (75) and eq. (78), depend only on the band gap $m(A)$, the band width ratio $J_0(A_i)/J_0(A_f)$, and the jump of the Chern number at the transition. The Chern number is, however, only defined in translationally in-

variant systems. Nevertheless, we expect our results to hold also for systems with weak disorder as we argue in the following. Note that this argument regards transitions that occur as a function of the parameter A in the presence of weak disorder. Disorder-driven topological transitions at intermediate or strong disorder as reported in Refs. [32, 33] are of different nature and, hence, not in the class of transitions we consider in this work.

Other than in undriven topological insulators edge modes of Floquet topological insulators can not only lie in the energy gap around $\epsilon_{\vec{k}} = 0$. Due to the periodicity of the quasi-energy spectrum they can also lie in the gap at $\epsilon_{\vec{k}} = \omega/2 = \pi/T$ that separates the quasi-energies of neighboring quasi-energy ‘‘Brillouin zones’’. The Chern number corresponds to the difference between the number of edge modes at $\epsilon = 0$, denoted by ν_0 , and the number of edge modes at $\epsilon = \pi/T$, denoted by ν_π , i.e. $C = \nu_0 - \nu_\pi$. In Ref. [20] a bulk invariant was introduced that directly corresponds to the number of edge states in a particular gap for systems with translational invariance. This was generalized to disordered systems in Ref. [34]. For the disordered system one adds additional time-independent fluxes $\vec{\Theta} = (\theta_x, \theta_y)$ threaded through the lattice to the time-periodic Hamiltonian of interest leading to a time evolution operator $U(\vec{\Theta}, t) = \mathcal{T}_{t'} \exp(-i \int_0^t dt' H(\vec{\Theta}, t'))$. The number of edge states in a gap around a given quasi-energy ϵ , ν_ϵ , is then determined by

$$\nu_\epsilon = W[U_\epsilon], \quad (82)$$

where

$$W[U_T] = \frac{1}{8\pi^2} \int_0^T dt \int d^2\theta \times \text{tr} \left(U_T^{-1} \partial_t U_T [U_T^{-1} \partial_{\theta_x} U_T, U_T^{-1} \partial_{\theta_y} U_T] \right) \quad (83)$$

is a winding number of the map $U_T(\vec{\Theta}, t)$ from $(\vec{\Theta}, t) \in S^1 \times S^1 \times S^1$ to the space of time evolution operators $U_T(\vec{\theta}, t)$ periodic in θ_x , θ_y , and t . $U_\epsilon(\vec{\Theta}, t)$ is related to the time evolution operator of the driven system $U(\vec{\Theta}, t)$ via

$$U_\epsilon(\vec{k}, t) = \begin{cases} U(\vec{\Theta}, 2t) & \text{if } 0 \leq t \leq T/2 \\ e^{-iH_{\text{eff}}^\epsilon(\vec{\Theta})t} & \text{if } T/2 \leq t \leq T \end{cases}. \quad (84)$$

In this expression ϵ determines the direction $e^{-i\epsilon T}$ of the branch cut of the logarithm in the definition of the effective Hamiltonian

$$H_{\text{eff}}^\epsilon(\vec{\Theta}) = \frac{i}{T} \log_\epsilon U(\vec{\Theta}, T). \quad (85)$$

With these results the characteristic non-analytic behavior given by eqs. (75) and (78) can be reexpressed in terms of the winding number W as

$$\sigma_{xy}^{\text{div.}} \sim \frac{\pi}{4} \text{sgn} \left(\frac{J_0(A_i)}{J_0(A_f)} \right) \left[\lim_{m_f \rightarrow 0^+} \Delta W - \lim_{m_f \rightarrow 0^-} \Delta W \right] \quad (86)$$

for quenches from the gapless initial state and as

$$\sigma_{xy}^{\text{div.}} \sim \frac{J_0(A_i)}{J_0(A_f^c)} \frac{\lim_{m_f \rightarrow 0^+} \Delta W - \lim_{m_f \rightarrow 0^-} \Delta W}{2|m_i|} \times \frac{dm_f}{dA_f} \Big|_{A_f=A_f^c} \ln |m_f| \quad (87)$$

for the gapped initial state. Here we introduced $\Delta W = W[U_0] - W[U_{\pi/T}]$. This form of the non-analytic behavior is expected to pertain also in the presence of weak disorder. Since beyond the scope of this work it is left for the future to demonstrate this anticipated behavior explicitly using specific examples.

Note, however, that these results for the non-analytic behavior apply only to transitions with conic gap closing points at $\epsilon = 0$, which corresponds to points \vec{q} in the Brillouin zone where the coefficient vector of the effective Hamiltonian vanishes, $|\vec{h}_{\vec{q}}| = 0$. A unique feature of Floquet systems is the possibility of gap closing points at $\epsilon = \pi/T$, which were for example studied in Refs. [17–20, 33]. These transitions correspond to the presence of points \vec{q} in the Brillouin zone where $|\vec{h}_{\vec{q}}| = \pi/T$. In that case any non-analyticity in the Hall conductance that is determined by the integral in eq. (62) must originate in non-analytic behavior of the numerator instead of roots of the denominator. Therefore, our analysis does not apply in these cases.

B. Conclusion

Based on a high frequency expansion of the effective Hamiltonian and the micromotion operator we studied the non-equilibrium Hall conductance after sudden switches of the driving amplitude. Considering a tight binding Hamiltonian on a hexagonal lattice with periodically modulated potential we found two kinds of non-analytic behavior after quenches close to critical driving amplitudes at which the ground state Chern number exhibits a jump. When the system is initially prepared in the undriven ground state of the gapless Hamiltonian H_0 the non-equilibrium Hall conductance jumps by $\pm \frac{\pi e^2}{2h}$ whenever the final driving amplitude A_f crosses a phase boundary A_c of the effective Hamiltonian with a gap-closing at the K -points. Considering neutral atoms in an optical lattice instead of an electronic system the electron charge e is to be replaced by unity. If the system is instead initially prepared in a Floquet mode of the driven Hamiltonian $H_{A_i}(t)$ the non-equilibrium Hall conductance after switching to A_f is continuous at $A_f = A_c$, but the derivative $\frac{d\sigma_{xy}}{dA_f}$ diverges logarithmically.

This non-analytic behavior is universal in the same sense as discussed in Ref. [16]. The characteristics of the non-analyticity only depend on the conic structure of the quasi-energy spectrum in the vicinity of the gap closing points and are therefore independent of other details of the model. In particular, it is expected that the behavior

remains the same in the presence of weak disorder, where the winding number of the time evolution operator serves as topological invariant instead of the Chern number.

Nevertheless, at the additional frequency dependent transition points visible in Fig. 3a one might find different behavior if the gap-closing points have different character. This question should be addressed in future research.

Our results show that the universal non-analytic behavior of the non-equilibrium Hall conductance carries over from closed TIs discussed in Refs. [15, 16] to FTIs, which can be realized experimentally in ultracold atom setups in optical lattices with the necessary control of external parameters [7, 35]. Moreover, small electric fields required to probe the Hall response can be generated in ultracold atom experiments [36]. These experiments naturally encounter a situation similar to the one considered in this work, because in the preparation process the external driving force is usually ramped up at some point in order to bring the system from the initial topologically trivial state into the topologically non-trivial state of the driven Hamiltonian. It is, however, understood, that the Chern number of a state is invariant under unitary evolution [9]. In a recent work [12] it was demonstrated how topological properties of the final Hamilto-

nian can nevertheless be inferred from the time-averaged non-equilibrium Hall conductance after slow but non-adiabatic ramps. Our results show that in the opposite limit of infinitely fast ramps the topological invariant determines the behavior close to transition points. In particular the jump height or the prefactor of the logarithmic divergence, respectively, are determined by the jump of the topological invariant at the transition. In future work it should be investigated, whether the behavior at infinitely long times investigated here can be found in the time-averaged Hall conductance at finite times similar to Ref. [12]. Moreover, the effect of ramping could be studied based on a high frequency expansion as presented in Ref. [37].

ACKNOWLEDGMENTS

The authors acknowledge helpful discussions with H. Dehghani, S. Kehrein, and D. Huse and thank L. Cevolani and N. Abeling for proof-reading the manuscript. M. Schmitt acknowledges support by the Studienstiftung des Deutschen Volkes. P. Wang is supported by NSFC under Grant No. 11304280. For the numerical computations the Armadillo library [38] was used.

-
- [1] K. v. Klitzing, G. Dorda, and M. Pepper, *Phys. Rev. Lett.* **45**, 494 (1980).
- [2] D. J. Thouless, M. Kohmoto, M. P. Nightingale, and M. den Nijs, *Phys. Rev. Lett.* **49**, 405 (1982).
- [3] F. D. M. Haldane, *Phys. Rev. Lett.* **61**, 2015 (1988).
- [4] M. Z. Hasan and C. L. Kane, *Rev. Mod. Phys.* **82**, 3045 (2010).
- [5] T. Oka and H. Aoki, *Phys. Rev. B* **79**, 081406 (2009).
- [6] T. Kitagawa, T. Oka, A. Brataas, L. Fu, and E. Demler, *Phys. Rev. B* **84**, 235108 (2011).
- [7] G. Jotzu, M. Messer, R. Desbuquois, M. Lebrat, T. Uehlinger, D. Greif, and T. Esslinger, *Nature* **515**, 237 (2014).
- [8] T. Kitagawa, E. Berg, M. Rudner, and E. Demler, *Phys. Rev. B* **82**, 235114 (2010).
- [9] L. D'Alessio and M. Rigol, *Nat. Commun.* **6**, 8336 (2015).
- [10] H. Dehghani, T. Oka, and A. Mitra, *Phys. Rev. B* **91**, 155422 (2015).
- [11] J. C. Budich and M. Heyl, *Phys. Rev. B* **93**, 085416 (2016).
- [12] Y. Hu, P. Zoller, and J. C. Budich, *Phys. Rev. Lett.* **117**, 126803 (2016).
- [13] M. D. Caio, N. R. Cooper, and M. J. Bhaseen, *Phys. Rev. B* **94**, 155104 (2016).
- [14] M. S. Rudner, N. H. Lindner, E. Berg, and M. Levin, *Phys. Rev. X* **3**, 031005 (2013).
- [15] P. Wang and S. Kehrein, *New Journal of Physics* **18**, 053003 (2016).
- [16] P. Wang, M. Schmitt, and S. Kehrein, *Phys. Rev. B* **93**, 085134 (2016).
- [17] T. Kitagawa, E. Berg, M. Rudner, and E. Demler, *Phys. Rev. B* **82**, 235114 (2010).
- [18] L. Jiang, T. Kitagawa, J. Alicea, A. R. Akhmerov, D. Pekker, G. Refael, J. I. Cirac, E. Demler, M. D. Lukin, and P. Zoller, *Phys. Rev. Lett.* **106**, 220402 (2011).
- [19] T. Kitagawa, M. A. Broome, A. Fedrizzi, M. S. Rudner, E. Berg, I. Kassal, A. Aspuru-Guzik, E. Demler, and A. G. White, *Nat. Commun.* **3**, 882 (2012).
- [20] M. S. Rudner, N. H. Lindner, E. Berg, and M. Levin, *Phys. Rev. X* **3**, 031005 (2013).
- [21] J. Karch, P. Olbrich, M. Schmalzbauer, C. Zoth, C. Brinsteiner, M. Fehrenbacher, U. Wurstbauer, M. M. Glazov, S. A. Tarasenko, E. L. Ivchenko, D. Weiss, J. Eroms, R. Yakimova, S. Lara-Avila, S. Kubatkin, and S. D. Ganichev, *Phys. Rev. Lett.* **105**, 227402 (2010).
- [22] A. Eckardt and E. Anisimovas, *New Journal of Physics* **17**, 093039 (2015).
- [23] M. Bukov, L. D'Alessio, and A. Polkovnikov, *Advances in Physics* **64**, 139 (2015).
- [24] G. Floquet, *Annales scientifiques de l'École Normale Supérieure* **12**, 47 (1883).
- [25] J. H. Shirley, *Phys. Rev.* **138**, B979 (1965).
- [26] N. Goldman and J. Dalibard, *Phys. Rev. X* **4**, 031027 (2014).
- [27] H. Sambe, *Phys. Rev. A* **7**, 2203 (1973).
- [28] F. N. Ünal, E. J. Mueller, and M. O. Oktel, *Phys. Rev. A* **94**, 053604 (2016).
- [29] S.-Q. Shen, *Topological Insulators* (Springer, Berlin, 2012).
- [30] R. M. Wilcox, *Journal of Mathematical Physics* **8**, 962 (1967).
- [31] P. Weinberg, M. Bukov, L. D'Alessio, A. Polkovnikov,

- S. Vajna, and M. Kolodrubetz, arXiv:1606.02229.
- [32] P. Titum, N. H. Lindner, M. C. Rechtsman, and G. Refael, *Phys. Rev. Lett.* **114**, 056801 (2015).
 - [33] S. Roy and G. J. Sreejith, *Phys. Rev. B* **94**, 214203 (2016).
 - [34] P. Titum, E. Berg, M. S. Rudner, G. Refael, and N. H. Lindner, *Phys. Rev. X* **6**, 021013 (2016).
 - [35] N. Fläschner, B. S. Rem, M. Tarnowski, D. Vogel, D.-S. Lühmann, K. Sengstock, and C. Weitenberg, *Science* **352**, 1091 (2016).
 - [36] M. Aidelsburger, M. Lohse, C. Schweizer, M. Atala, J. T. Barreiro, S. Nascimbene, N. R. Cooper, I. Bloch, and N. Goldman, *Nat. Phys.* **11**, 162 (2015).
 - [37] V. Novičenko, E. Anisimovas, and G. Juzeliūnas, *Phys. Rev. A* **95**, 023615 (2017).
 - [38] C. Sanderson and R. Curtin, *Journal of Open Source Software* **1**, 26 (2016).
 - [39] T. Fukui, Y. Hatsugai, and H. Suzuki, *Journal of the Physical Society of Japan* **74**, 1674 (2005).

Appendix A: Restoring translational invariance by a time-dependent gauge transformation

In order to restore translational invariance we perform a time-dependent gauge transformation with

$$W(t) = \prod_i \exp\left(i c_i^\dagger c_i \int dt V(\vec{r}_i, t) \right) \quad (\text{A1})$$

yielding

$$\begin{aligned} H(t) &= W(t) \tilde{H}(t) W^\dagger(t) - iW(t) \partial_t W^\dagger(t) \\ &= -J \sum_{\langle i,j \rangle} \left(e^{-i\theta_{ij}(t)} c_i^\dagger c_j + h.c. \right), \end{aligned} \quad (\text{A2})$$

where

$$\theta_{ij}(t) = (\vec{r}_i - \vec{r}_j) \cdot \vec{A}(t) \quad (\text{A3})$$

was introduced with

$$\vec{A}(t) = \frac{V_0 a}{\omega} \begin{pmatrix} \sin(\omega t) \\ \cos(\omega t) \end{pmatrix}, \quad (\text{A4})$$

where a denotes the lattice spacing.

Introducing explicit labels A and B for the sublattices and the Fourier transform of the operators,

$$c_{i,A/B} = \frac{1}{\sqrt{N}} \sum_{\vec{k}} e^{-i\vec{k} \cdot \vec{r}_{i,A/B}} c_{\vec{k},A/B} \quad (\text{A5})$$

yields the Hamiltonian in momentum space,

$$H(t) = -J \sum_{\vec{k}} \vec{c}_{\vec{k}}^\dagger \left[\vec{d}_{\vec{k}}(t) \cdot \vec{\sigma} \right] \vec{c}_{\vec{k}}. \quad (\text{A6})$$

In this expression for the Hamiltonian we introduced

$$\vec{c}_{\vec{k}} = \begin{pmatrix} c_{\vec{k}A} \\ c_{\vec{k}B} \end{pmatrix} \quad (\text{A7})$$

and the coefficient vector $\vec{d}_{\vec{k}}(t)$ is given in eqs. (4)-(6) in the main text.

Appendix B: Numerical computation of Floquet modes and Hall conductance

In order to solve eq. (25) numerically we set up the matrix Q as given in eq. (26) truncating it at some maximal $|m| = M$. The diagonalization of the truncated matrix yields Floquet modes $|\phi_{nm}\rangle$ for $-M \leq m \leq M$ and corresponding quasi-energies with the property $\epsilon_{nm} = \epsilon_{n0} + m\omega$ for small $|m|$. The best approximation for the eigenvector of the infinite matrix is obtained in the middle of the spectrum, i.e. for $m = 0$.

For the two-band system under consideration we obtain a solution at every \vec{k} -point and the solutions can be written as vectors with $2(2M+1)$ components

$$\vec{\phi}_{\vec{k},M}^{\alpha m} \equiv |\phi_{\vec{k}}^{\alpha m}\rangle = \begin{pmatrix} \phi_{\vec{k},(u,M)}^{\alpha m} \\ \phi_{\vec{k},(d,M)}^{\alpha m} \\ \phi_{\vec{k},(u,M-1)}^{\alpha m} \\ \vdots \\ \phi_{\vec{k},(d,-M)}^{\alpha m} \end{pmatrix} \quad (\text{B1})$$

The best approximation to the time-dependent Floquet mode $|u_{\vec{k}}^\alpha(t)\rangle \in \mathbb{C}^2$ is then given by

$$|\phi_{\vec{k}}^\alpha(t)\rangle = \sum_{\beta \in \{u,d\}} \sum_{n=-M}^M e^{in\omega t} \phi_{\vec{k},(\beta,n)}^{\alpha 0} |\beta\rangle. \quad (\text{B2})$$

Plugging eq. (B2) into eq. (34) yields

$$\begin{aligned} \bar{F}_{\vec{k}} &= \int_0^T \frac{dt}{T} \sum_{\alpha,\alpha'} \sum_{n,n'} \langle \alpha | e^{-in\omega t} \partial_x (\phi_{\vec{k},(\alpha,n)}^{d0})^* \partial_y (\phi_{\vec{k},(\alpha',n')}^{d0}) e^{in'\omega t} | \alpha' \rangle \\ &= \sum_{\alpha,\alpha'} \sum_{n,n'} \partial_x (\phi_{\vec{k},(\alpha,n)}^{d0})^* \partial_y (\phi_{\vec{k},(\alpha',n')}^{d0}) \underbrace{\langle \alpha | \alpha' \rangle}_{\delta_{\alpha\alpha'}} \underbrace{\int_0^T \frac{dt}{T} e^{i(n'-n)\omega t}}_{\delta_{nn'}} \\ &= \sum_{\alpha} \sum_n \partial_x (\phi_{\vec{k},(\alpha,n)}^{d0})^* \partial_y (\phi_{\vec{k},(\alpha,n)}^{d0}) = \left(\partial_x \vec{\phi}_{\vec{k},M}^{d0} \right) \cdot \left(\partial_y \vec{\phi}_{\vec{k},M}^{d0} \right) \end{aligned} \quad (\text{B3})$$

This means it is not necessary to perform the time-averaging for the averaged Berry curvature explicitly. The derivatives can be approximated as difference quotients. This procedure yields a numerical approximation

for $\bar{F}_{\vec{k}}$ on a grid of \vec{k} -points. Choosing this grid appropriately the Hall conductance (33) can be computed efficiently using the method introduced in Ref. [39] as already established by Dehghani et al. [10].

Appendix C: Derivation of time dependent mode occupation numbers

The first order term of the high frequency expansion of the kick operator is

$$\mathcal{K}^{(1)}(t) = -i \sum_{m=1}^{\infty} \frac{e^{im\omega t} H_m - e^{-im\omega t} H_{-m}}{m} \quad (\text{C1})$$

Note that in this fomula we dropped the explicit \vec{k} -dependence in the notation, which we will do also in the rest of this section wherever it is not relevant in order to keep the notation clear.

We approximate the micromotion operator with

$$U_F(t) = \exp\left(-i\mathcal{K}^{(1)}(t)/\omega\right) + \mathcal{O}(\omega^{-2}) \quad (\text{C2})$$

and define $\vec{g}(t) = (g_x(t), g_y(t), g_z(t))$ via

$$-\mathcal{K}^{(1)}(t) = g_x(t)\sigma^x + g_y(t)\sigma^y + g_z(t)\sigma^z. \quad (\text{C3})$$

Note that according to eq. (C1) $g_z(t) = 0$ to first order in $1/\omega$. The expression for $\mathcal{K}^{(1)}(t)$ as sum of Pauli matrices allows to rewrite the micromotion operator as

$$\begin{aligned} \exp\left(-i\mathcal{K}^{(1)}(t)\right) &= \exp\left[ig(t)(\vec{n}(t) \cdot \vec{\sigma})\right] \\ &= \cos(g(t)) + i \sin(g(t))(\vec{n}(t) \cdot \vec{\sigma}) \end{aligned} \quad (\text{C4})$$

with

$$\vec{n}(t) = \frac{\vec{g}(t)}{g(t)}, \quad g(t) = |\vec{g}(t)|. \quad (\text{C5})$$

Plugging this expression for the micromotion operator into eq. (21) we obtain the overlaps of Floquet modes,

$$\langle \phi_0^d(t) | \phi^\alpha(t) \rangle = \langle u_0^d | [\cos(g_0(t)) - i \sin(g_0(t))(\vec{n}_0 \cdot \vec{\sigma})] [\cos(g(t)) + i \sin(g(t))(\vec{n} \cdot \vec{\sigma})] | u^\alpha \rangle \quad (\text{C6})$$

$$\begin{aligned} &= \langle u_0^d | u^\alpha \rangle \cos(g_0(t)) \cos(g(t)) + \sin(g_0(t)) \sin(g(t)) \langle u_0^d | (\vec{n}_0 \cdot \vec{\sigma})(\vec{n} \cdot \vec{\sigma}) | u^\alpha \rangle \\ &\quad - i \sin(g_0(t)) \cos(g(t)) \langle u_0^d | \vec{n}_0 \cdot \vec{\sigma} | u^\alpha \rangle + i \cos(g_0(t)) \sin(g(t)) \langle u_0^d | \vec{n} \cdot \vec{\sigma} | u^\alpha \rangle \end{aligned} \quad (\text{C7})$$

where the index 0 indicates Floquet modes/micromotion operator of the initial Hamiltonian with driving amplitude A_0 . To evaluate this we need the eigenstates of the effective Hamiltonian $H_{F\vec{k}} = \vec{h}_{\vec{k}} \cdot \vec{\sigma}$, which read

$$|u_{\vec{k}}^{u/d}\rangle = \sqrt{\frac{h_{\vec{k}x}^2 + h_{\vec{k}y}^2}{2|\vec{h}_{\vec{k}}|(|\vec{h}_{\vec{k}}| \pm h_{\vec{k}z})}} \begin{pmatrix} \frac{h_{\vec{k}z} \pm |\vec{h}_{\vec{k}}|}{h_{\vec{k}x} + ih_{\vec{k}y}} \\ 1 \end{pmatrix}. \quad (\text{C8})$$

These yield the overlaps

$$\Gamma_1^\alpha \equiv \langle u_0^d | u^\alpha \rangle = \frac{1 + \frac{h_z^0 - |\vec{h}_0|}{h_x^0 - ih_y^0} \frac{h_z \pm |\vec{h}|}{h_x + ih_y}}{\mathcal{N}_\alpha} \quad (\text{C9})$$

$$\Gamma_x^\alpha \equiv \langle u_0^d | \sigma^x | u^\alpha \rangle = \frac{\frac{h_z^0 - |\vec{h}_0|}{h_x^0 - ih_y^0} + \frac{h_z \pm |\vec{h}|}{h_x + ih_y}}{\mathcal{N}_\alpha} \quad (\text{C10})$$

$$\Gamma_y^\alpha \equiv \langle u_0^d | \sigma^y | u^\alpha \rangle = -i \frac{\frac{h_z^0 - |\vec{h}_0|}{h_x^0 - ih_y^0} - \frac{h_z \pm |\vec{h}|}{h_x + ih_y}}{\mathcal{N}_\alpha} \quad (\text{C11})$$

where

$$\mathcal{N}_\alpha^{-1} = \sqrt{\frac{(h_x^2 + h_y^2)(h_x^{02} + h_y^{02})}{4|\vec{h}_0||\vec{h}|(|\vec{h}_0| - h_z^0)(|\vec{h}| \pm h_z)}} \quad (\text{C12})$$

Then

$$\begin{aligned} \langle \phi_0^d(t) | \phi^\alpha(t) \rangle &= \Gamma_1^\alpha [\cos(g_0) \cos(g) + \sin(g_0) \sin(g)(n_0^x n^x + n_0^y n^y)] \\ &\quad + i \Gamma_z^\alpha \sin(g_0) \sin(g)(n_0^x n^y - n_0^y n^x) \\ &\quad - i \sin(g_0) \cos(g)(n_0^x \Gamma_x^\alpha + n_0^y \Gamma_y^\alpha) \\ &\quad + i \cos(g_0) \sin(g)(n^x \Gamma_x^\alpha + n^y \Gamma_y^\alpha) \\ &= \Gamma_1^\alpha [\cos(g_0) \cos(g) + \sin(g_0) \sin(g)(n_0^x n^x + n_0^y n^y)] \\ &\quad + i \Gamma_y^\alpha (\cos(g_0) \sin(g) n^y - \sin(g_0) \cos(g) n_0^y) \\ &\quad + i \Gamma_x^\alpha (\cos(g_0) \sin(g) n^x - \sin(g_0) \cos(g) n_0^x) \\ &\quad + i \Gamma_z^\alpha \sin(g_0) \sin(g)(n_0^x n^y - n_0^y n^x) \end{aligned} \quad (\text{C13})$$

Since $g, g_0 \sim \mathcal{O}(\omega^{-1})$, we approximate $\cos(g) \approx 1$ and $\sin(g) \approx g$ and drop all terms of $\mathcal{O}(\omega^{-2})$, which yields

$$\begin{aligned} \langle \phi_0^d(t) | \phi^\alpha(t) \rangle &= \Gamma_1^\alpha + i \Gamma_y^\alpha (g(t) n^y(t) - g_0(t) n_0^y(t)) \\ &\quad + i \Gamma_x^\alpha (g(t) n^x(t) - g_0(t) n_0^x(t)) \\ &= \Gamma_1^\alpha + i \Gamma_y^\alpha \underbrace{(g_y(t) - g_y^0(t))}_{\equiv \Delta g_y(t)} + i \Gamma_x^\alpha \underbrace{(g_x(t) - g_x^0(t))}_{\equiv \Delta g_x(t)} \end{aligned} \quad (\text{C14})$$

Then, again omitting terms quadratic in $1/\omega$,

$$\begin{aligned} & |\langle \phi_0^d(t) | \phi^\alpha(t) \rangle|^2 \\ &= (\Gamma_1^\alpha + i\Gamma_y^\alpha \Delta g_y(t) + i\Gamma_x^\alpha \Delta g_x(t)) \\ &\quad \times (\Gamma_1^{\alpha*} - i\Gamma_y^{\alpha*} \Delta g_y(t) - i\Gamma_x^{\alpha*} \Delta g_x(t)) \\ &= |\Gamma_1^\alpha|^2 - \text{Im}[\Gamma_1^{\alpha*} \Gamma_x^\alpha] \Delta g_x(t) - \text{Im}[\Gamma_1^{\alpha*} \Gamma_y^\alpha] \Delta g_y(t) \end{aligned} \quad (\text{C15})$$

In the end we are interested in

$$\begin{aligned} & |\langle \phi_0^d(t) | \phi^d(t) \rangle|^2 - |\langle \phi_0^d(t) | \phi^u(t) \rangle|^2 \\ &= (|\Gamma_1^d|^2 - |\Gamma_1^u|^2) \\ &\quad - (\text{Im}[\Gamma_1^{d*} \Gamma_x^d] - \text{Im}[\Gamma_1^{u*} \Gamma_x^u]) \Delta g_x(t) \\ &\quad - (\text{Im}[\Gamma_1^{d*} \Gamma_y^d] - \text{Im}[\Gamma_1^{u*} \Gamma_y^u]) \Delta g_y(t) \end{aligned} \quad (\text{C16})$$

The different contributions to the overlaps are

$$|\Gamma_1^d|^2 - |\Gamma_1^u|^2 = \frac{\vec{d}_0 \cdot \vec{d}}{|d||d_0|} \quad (\text{C17})$$

$$\text{Im}[\Gamma_1^{d*} \Gamma_x^d] - \text{Im}[\Gamma_1^{u*} \Gamma_x^u] = \frac{d_y d_z^0 - d_y^0 d_z}{|d||d_0|} \quad (\text{C18})$$

$$\text{Im}[\Gamma_1^{d*} \Gamma_y^d] - \text{Im}[\Gamma_1^{u*} \Gamma_y^u] = \frac{d_x^0 d_z - d_x d_z^0}{|d||d_0|} \quad (\text{C19})$$

Since $\Delta g_z(t) = 0$, we can finally write

$$\begin{aligned} & |\langle \phi_0^d(t) | \phi^d(t) \rangle|^2 - |\langle \phi_0^d(t) | \phi^u(t) \rangle|^2 \\ &= \frac{\vec{h}_0 \cdot \vec{h}}{|h||h_0|} + \frac{(\vec{h}_0 \times \vec{h}) \cdot \Delta \vec{g}(t)}{|h||h_0|} + \mathcal{O}(\omega^{-2}). \end{aligned} \quad (\text{C20})$$

Appendix D: Partially filled bands

In this section we derive the leading contribution to

$$\begin{aligned} & \sin(2\theta_{\vec{k}}) \text{Re} \left[e^{i\varphi_{\vec{k}}(t)} \left(\langle \phi_{0\vec{k}}^d(t) | \phi_{\vec{k}}^d(t) \rangle \langle \phi_{\vec{k}}^d(t) | \phi_{0\vec{k}}^u(t) \rangle \right. \right. \\ & \quad \left. \left. - \langle \phi_{0\vec{k}}^d(t) | \phi_{\vec{k}}^u(t) \rangle \langle \phi_{\vec{k}}^u(t) | \phi_{0\vec{k}}^u(t) \rangle \right) \right] \end{aligned} \quad (\text{D1})$$

which is a part of the occupation difference when quenching from partially filled Floquet bands given in eq. (80) in the main text. For the sake of brevity we will drop the explicit \vec{k} -dependence in the notation wherever it is not relevant in the following.

The derivation is analogous to the one given in appendix C. We generalise the expressions for the overlaps

(C9)-(C11) to

$$\Gamma_1^{\alpha\beta} = \langle u_0^\alpha | u^\beta \rangle = \frac{1}{\mathcal{N}_{\alpha\beta}} \left(1 + \frac{h_z^0 \pm h_0}{h_x^0 - ih_y^0} \frac{h_z \pm h}{h_x + ih_y} \right) \quad (\text{D2})$$

$$\Gamma_x^{\alpha\beta} = \langle u_0^\alpha | \sigma^x | u^\beta \rangle = \frac{1}{\mathcal{N}_{\alpha\beta}} \left(\frac{h_z^0 \pm h_0}{h_x^0 - ih_y^0} + \frac{h_z \pm h}{h_x + ih_y} \right) \quad (\text{D3})$$

$$\Gamma_y^{\alpha\beta} = \langle u_0^\alpha | \sigma^y | u^\beta \rangle = -i \frac{1}{\mathcal{N}_{\alpha\beta}} \left(\frac{h_z^0 \pm h_0}{h_x^0 - ih_y^0} - \frac{h_z \pm h}{h_x + ih_y} \right) \quad (\text{D4})$$

with

$$\mathcal{N}_{\alpha\beta} = \sqrt{\frac{(h_x^2 + h_y^2)(h_x^0{}^2 + h_y^0{}^2)}{4hh_0(h_0 \pm h_z^0)(h \pm h_z)}}. \quad (\text{D5})$$

In the expressions above α is always associated with the first \pm and β with the second. For the overlaps in eq. (D1) this yields

$$\begin{aligned} & \langle \phi_{0\vec{k}}^d(t) | \phi_{\vec{k}}^d(t) \rangle \langle \phi_{\vec{k}}^d(t) | \phi_{0\vec{k}}^u(t) \rangle - \langle \phi_{0\vec{k}}^d(t) | \phi_{\vec{k}}^u(t) \rangle \langle \phi_{\vec{k}}^u(t) | \phi_{0\vec{k}}^u(t) \rangle \\ &= \left(\Gamma_1^{dd} + i\Gamma_x^{dd} \Delta g_x(t) + i\Gamma_y^{dd} \Delta g_y(t) \right) \\ &\quad \times \left(\Gamma_1^{ud*} - i\Gamma_x^{ud*} \Delta g_x(t) - i\Gamma_y^{ud*} \Delta g_y(t) \right) \\ &\quad - \left(\Gamma_1^{du} + i\Gamma_x^{du} \Delta g_x(t) + i\Gamma_y^{du} \Delta g_y(t) \right) \\ &\quad \times \left(\Gamma_1^{uu*} - i\Gamma_x^{uu*} \Delta g_x(t) - i\Gamma_y^{uu*} \Delta g_y(t) \right) \\ &= \frac{h_z^0(h_x^0 h_x + h_y^0 h_y) + ih_0(h_x^0 h_y - h_y^0 h_x)}{hh_0 \sqrt{h_x^0{}^2 + h_y^0{}^2}} \\ &\quad - \frac{4h_z}{hh_0 \sqrt{h_x^0{}^2 + h_y^0{}^2}} \left[h_z^0 h_y^0 + ih_0 h_x^0 \right] \Delta g_x(t) \\ &\quad + \frac{4h_z}{hh_0 \sqrt{h_x^0{}^2 + h_y^0{}^2}} \left[h_z^0 h_x^0 - ih_0 h_y^0 \right] \Delta g_y(t) + \mathcal{O}(\omega^{-2}) \end{aligned} \quad (\text{D6})$$

where second order terms were omitted.

We consider the first term, which is frequency independent. When the linearisation around the gap closing point given in eqs. (63)-(65) is plugged in, the imaginary part vanishes. For the real part we can approximate $h_0 \approx h_0^z$ close to the gap closing point. Thereby we obtain

$$\frac{h_x^0 h_x + h_y^0 h_y}{h \sqrt{h_x^0{}^2 + h_y^0{}^2}} \quad (\text{D7})$$

The contribution of this part of the occupation to the

Hall conductance is

$$\begin{aligned} \sigma_{xy}^{(2)} = & \int \frac{d^2k}{4\pi} \sin(2\theta_{\vec{k}}) \cos(\varphi_{\vec{k}}(t)) \\ & \times \frac{h_{\vec{k}x}^0 h_{\vec{k}x} + h_{\vec{k}y}^0 h_{\vec{k}y}}{\sqrt{h_{\vec{k}x}^0{}^2 + h_{\vec{k}y}^0{}^2}} \frac{(\partial_x \vec{h}_{\vec{k}} \times \partial_y \vec{h}_{\vec{k}}) \vec{h}_{\vec{k}}}{h_{\vec{k}}^4} \end{aligned} \quad (\text{D8})$$

Assuming $\sin(2\theta_{\vec{k}}) \cos(\varphi_{\vec{k}}(t))$ well behaved in the vicinity of the gap closing point \vec{k}_0 , we can approximate

$$\begin{aligned} \sigma_{xy}^{(2)} = & \sin(2\theta_{\vec{k}_0}) \cos(\varphi_{\vec{k}_0}(t)) \\ & \times \int \frac{d^2k}{4\pi} \frac{h_{\vec{k}x}^0 h_{\vec{k}x} + h_{\vec{k}y}^0 h_{\vec{k}y}}{\sqrt{h_{\vec{k}x}^0{}^2 + h_{\vec{k}y}^0{}^2}} \frac{(\partial_x \vec{h}_{\vec{k}} \times \partial_y \vec{h}_{\vec{k}}) \vec{h}_{\vec{k}}}{h_{\vec{k}}^4} \end{aligned} \quad (\text{D9})$$

and then the integral is the same one gets when quenching from a gapless initial state, which is discussed in section III C 1 of the main text. This means, that partially filled initial states add a jump to the Hall conductance at the transition. But through the $\cos(\varphi_{\vec{k}_0}(t))$ factor the jump oscillates as function of the quench time with frequency equal to the initial gap $2m(A_i)$.

